AgBioForum, 26(3): 119-127. ©2024 ***AgBioForum***

Assessing Temperature Regulation for Roof Full-Open Glass Greenhouse in Yangtze River Delta: A Time Series Comparison and CFD Method Approach

ZHANG WEIJIAN
School of Mechanical Engineering, College of Engineering, Universiti Teknologi MARA, Selangor, Malaysia.
Email: m15751010257@163.com

Nurnida Elmira Binti Othman*
School of Mechanical Engineering, College of Engineering, Universiti Teknologi MARA, Selangor, Malaysia.
Email: nurnida@uitm.edu.my

Azli Bin Abd Razak
School of Mechanical Engineering, College of Engineering, Universiti Teknologi MARA, Selangor, Malaysia.
Email: azlirazak@uitm.edu.my

The Yangtze River Delta (YRD) is a densely populated region where the advancement of efficient and intensive agricultural practices is crucial. Glass greenhouses, particularly in areas such as Shanghai, frequently become unusable during the summer months due to excessive internal temperatures, primarily resulting from inadequate knowledge of cooling techniques. This study employs a time series comparative approach to evaluate the cooling performance under seven different operational conditions, utilising Computational Fluid Dynamics (CFD) to simulate and illustrate the greenhouse characteristics when subjected to external wind forces specific to the YRD. The findings reveal that, in glass greenhouses lacking side windows, the internal temperature distribution during summer—under the prevailing southerly wind conditions—exhibits a general pattern of lower temperatures in the south and west, and higher temperatures in the north and east. This indicates that the southwest quadrant achieves the most effective cooling, whereas the northeast quadrant performs poorly in this regard. Moreover, mechanical ventilation proved significantly more effective than natural ventilation, achieving a cooling reduction of up to 4.02°C compared to 1.53°C in naturally ventilated greenhouses. Natural ventilation still outperformed conditions with no ventilation at all. In addition, the implementation of multi-layer shading nets demonstrated notable cooling benefits. When outdoor radiation exceeded 800 W/m², the use of two shading layers achieved a temperature reduction of 4.5°C, whereas a single layer provided a reduction of 3.7°C in experimental settings. Based on these analyses, the study proposes specific strategies for the utilisation of glass greenhouses under the summer climatic conditions typical of the Yangtze River Delta.

Keywords: Greenhouse, Temperature Regulation, Time Series Comparison, CFD, Yangtze River Delta Region.

Introduction

The YRD region is a triangular megacity that generally comprises Shanghai, southern Jiangsu, and northern Zhejiang. This area lies at the core of the southern section of the Yangtze River. Rapid urbanisation within the region has resulted in a globally significant agglomeration of metropolitan areas. Spanning approximately 350,000 square kilometres, the YRD is home to over 240 million individuals. Given the high population density, the promotion of efficient and sustainable greenhouse agriculture is of particular importance in this region (Fan et al., 2023). Currently, greenhouses in the YRD experience severe internal heat accumulation during the summer, rendering many unusable due to insufficient knowledge regarding effective cooling regulation methods. This situation leads to resource inefficiencies, especially in light of increasing pressure on food supply chains (Wang Xinzhong, 2016). Therefore, investigating the thermal regulation mechanisms within greenhouses during the summer in the YRD and establishing appropriate cooling strategies is of considerable practical value. Such studies also offer theoretical guidance for greenhouse design and operational improvement.

During summer under hot and humid climatic conditions, commonly employed cooling techniques in greenhouses include wet curtain-fan systems, circulation fans, shading nets, natural ventilation, and other related approaches (Ganguly & Ghosh, 2011). Substantial research has been undertaken concerning the application of these methods under various climatic scenarios (Badji et al., 2022). One study examined mechanical ventilation by combining practical experimentation with CFD-based simulations, demonstrating that the height of fan installation significantly affects the extent of the cooling zone, with diminished effectiveness beyond that height (Flores-Velazquez et al., 2014). Another investigation indicated a direct relationship between fan power and cooling efficiency—greater power resulted in a more substantial reduction in indoor temperature relative to external conditions (Ghani et al., 2020). Further work explored the nuanced impacts of mechanical ventilation by testing four different inlet air velocities and analysing their influence on parameters such as temperature gradients, air velocity fields, direct irradiation patterns, and static pressure distribution within agricultural greenhouses (Chiboub et al., 2024).

In relation to natural ventilation, findings have shown that the combined use of side and roof vents leads to improved ventilation efficiency, outperforming setups utilising only side or roof openings (Villagrán et al., 2021). Another study investigating ventilation and cooling in continuous gable plastic greenhouses revealed that factors such as side vent aperture and crop height considerably affect the

internal microclimate (Lyu et al., 2022). Additional researchers have observed that temperature distribution in greenhouses is often affected by the choice of ventilation strategy, with natural ventilation outcomes strongly influenced by prevailing wind directions (Wang et al., 2021).

Studies on shading nets have demonstrated that such installations not only reduce incoming solar radiation but also enhance cooling capacity and retain internal humidity, thus maintaining greenhouse conditions suitable for crop development even during periods of high external temperature (Ahmed et al., 2019). Further evidence indicates that shading nets also help to regulate temperature and humidity inside the greenhouse, thereby optimising the internal environment for plant growth (Nomura et al., 2022). Time series analysis has also been applied in greenhouse studies, particularly for forecasting and comparative assessments, confirming its widespread adoption in this domain (Ali & Hassanein, 2020; Cao et al., 2023; Ludwig, 2019). Moreover, CFD techniques have gained prominence in recent years as a key methodology in the study of greenhouse dynamics (Choi, Kim, & Lee, 2024; Feng et al., 2024).

Despite the extensive research into cooling systems and ventilation methods, it is important to acknowledge that greenhouses exhibit region-specific characteristics, especially due to climatic variability. As such, the introduction of modern agricultural greenhouses into new regions requires tailored research to ensure the development of effective and context-specific management strategies.

Experimental Setup and Procedure

In the YRD region, glass greenhouses are often rendered inoperative during the summer months due to the absence of effective cooling strategies. This study aims to examine the regulatory factors influencing greenhouse environments during summer and to conduct experimental investigations into temperature distribution by modifying operational parameters such as ventilation systems and shading nets. Time series analysis, which involves data points arranged in chronological sequence, facilitates a comparative evaluation of the impact of multiple operational configurations on a consistent test environment. In this context, temperature represents a critical variable influencing plant growth within greenhouses. Accordingly, time series experiments focusing on ventilation regulation and shading net configurations were implemented. Experimental data were analysed using a comparative algorithm and CFD simulation to identify patterns in internal temperature regulation. Based on these findings, a strategic framework for greenhouse operation during the summer months in the YRD region was proposed. The overall study design is illustrated in Figure 1.

The CFD simulations conducted in this research are based on steady-state analysis, incorporating energy equations, turbulence models, and radiation models, with a primary emphasis on temperature variation. Owing to inherent limitations within computational fluid dynamics, a degree of discrepancy between simulation outcomes and actual environmental conditions is inevitable. Furthermore, as this study primarily utilises meteorological data specific to the YRD, and given that greenhouse performance is influenced by regional environmental variables, the findings provide theoretical guidance applicable predominantly to this geographical context.

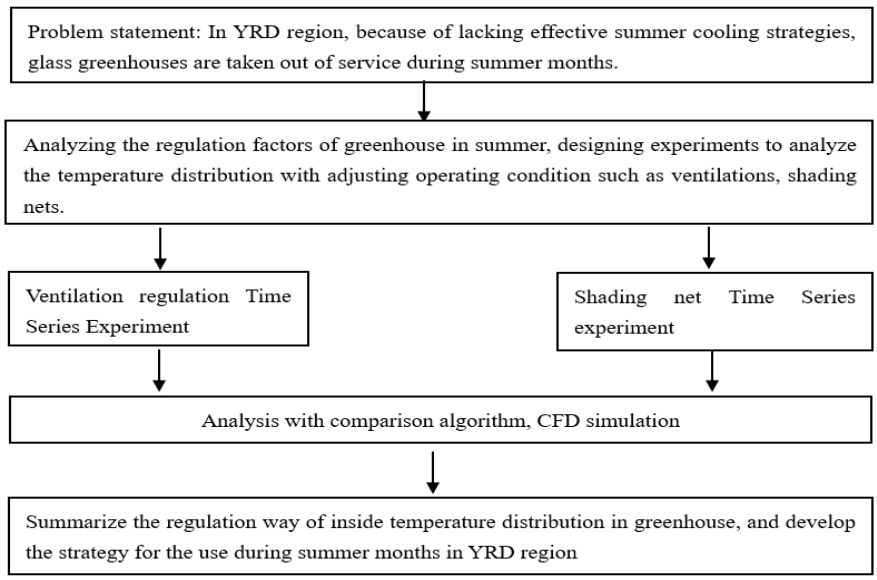

Figure 1: Overall Research Framework.

Experiment Object

A one-span, three-roof, fully open glass greenhouse located in Ye Yuan (9166 Caolang Highway, Jinshan District, Shanghai, China) was selected as the subject of this study, as depicted in Figure 2. The greenhouse is geographically situated at 119.78°E and 31.7°N, within the subtropical monsoon climatic zone (Fan et al., 2023), the primary framework of the greenhouse comprises structural steel, while the surrounding enclosure consists of double-layered hollow float glass. The roof features a fully open skylight design, with two layers of mesh internal shading nets installed at the top. The greenhouse ridge is aligned along the north–south axis, as depicted in Figure 3.

Exhaust fans were mounted on the northern wall, whereas wet curtains were positioned on the southern wall. Circular flow fans were vertically arranged within the interior, with an installation height of approximately 2 metres. Notably, the east and west walls of the greenhouse were constructed without side windows.

Figure 2: The Roof Full-Open Greenhouse

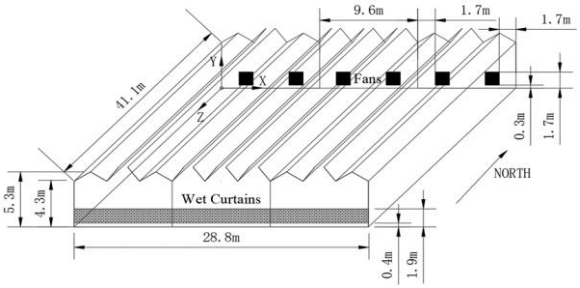

Figure 3: Schematic View of Simulated Greenhouse.

Layout of Measurement Points and Selection of Instruments

According to previous research (Odhiambo et al., 2020), solar radiation in the YRD region, including Shanghai, reaches its peak during July and August. The present experiment was conducted in early August, characterised by intense solar radiation and representing typical hot summer conditions in the YRD region. Indoor temperature within the greenhouse was monitored using ZDR-3W1S automatic temperature recorders (temperature measurement range: −40 to 100 °C, accuracy: ± 0.1 °C; humidity measurement range: 0 to 100% RH, accuracy: ±3% RH). The crop height in the experimental greenhouses generally ranged between 0.4 and 1.5 m. Considering the prevalent features of greenhouse cultivation in the YRD region (Ganguly & Ghosh, 2011), heights of 0.7 m and 1.3 m were selected to represent typical plant growth stages, with greater emphasis placed on the 0.7 m level. A height of 2.1 m was chosen to represent the upper region of the greenhouse. Temperature sensors were arranged within the central section of the greenhouse, comprising a total of 21 measurement points. The sensor layout formed two intersecting vertical planes, as illustrated in Figure 4. Each sensor was designated using the label *i*, where the value of *i* corresponds to a natural number from 1 to 21. The positional coordinates of each sensor within the defined coordinate system are detailed in Table 1.

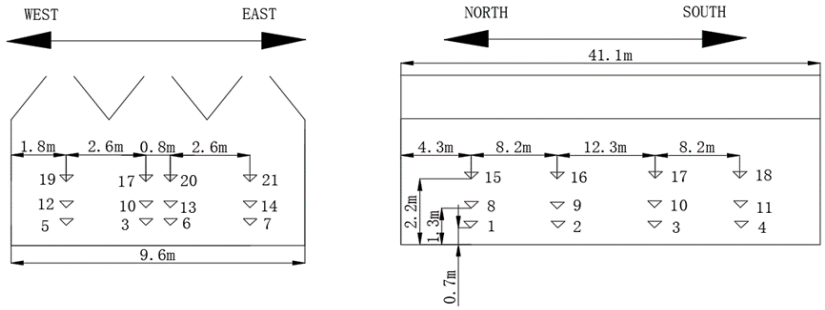

Figure 4: Sensor Locations Formed Two Crossed Vertical Planes.

Table 1: The Coordinates of the Temperature Sensors Setting in Greenhouse.

Code:*i*	*X* /m	*Y* /m	*Z* /m	Code:*i*	*X* /m	*Y* /m	*Z* /m
1	14	0.7	4.3	13	14.8	1.3	24.8
2	14	0.7	12.5	14	17.4	1.3	24.8
3	14	0.7	24.8	15	14	2.2	4.3
4	14	0.7	33	16	14	2.2	12.5
5	11.4	0.7	24.8	17	14	2.2	24.8
6	14.8	0.7	24.8	18	14	2.3	33
7	17.4	0.7	24.8	19	11.4	2.2	24.8
8	14	1.3	4.3	20	14.8	2.2	24.8
9	14	1.3	12.5	21	17.4	2.2	24.8
10	14	1.3	24.8				
11	14	1.3	33				
12	11.4	1.3	24.8				

The weather station employed in the experiment is an ultrasonic automatic weather station manufactured by Beijing Tian-Yu-De Company. The instrument used was a TYD-ZS2 environmental data logger, with a temperature measurement accuracy of ±0.1 °C and a measurement range of −40 to 80 °C. The wind speed accuracy is 0.1 m/s, with a measurement range of 0 to 70 m/s, while the wind direction accuracy is 1°, with a measurement range of 0 to 360°. The weather station was positioned outside, 3 metres from the northern wall, to monitor fluctuations in outdoor temperature, as shown in Figure 5.

Figure 5: The Weather Station Instrument Set Up at Outdoor Condition.

Experiment Methods: Ventilation Time Series Experiment and Analysis

The data were collected from two sets of time series experiments. The basic conditions of the greenhouse during the experiments were as follows: the rear cover of the fan on the northern wall was opened to allow external airflow to enter the greenhouse through the fan opening, while the ventilation openings of the wet curtains on the southern wall served as vents. The skylight was opened to an angle of 52.4°, and the three roof skylights of the middle span of the greenhouse were fully opened. In contrast, only the small roof skylight in the middle was opened in the other two spans of the greenhouse. The time series experiment for ventilation was conducted as follows: the TYD-ZS2 weather station (environmental data logger) was set to collect one group of temperature data every minute. The time series for three states were measured in the following order: 1) no ventilation, 2) natural ventilation, and 3) fan and wet-curtain ventilation. The values of c for these four operating conditions were 1, 2, 3, and 4, respectively. The ZDR-3W1S devices were automatically calibrated and set to the automatic measurement mode, recording data every 5 minutes. The measurement time for each condition was 20 minutes, with 5 sets of values recorded for each condition. A 10-minute interval between conditions was allowed to adjust the greenhouse equipment and stabilise the environment for the next condition. The specific measurement steps are illustrated in Figure 6.

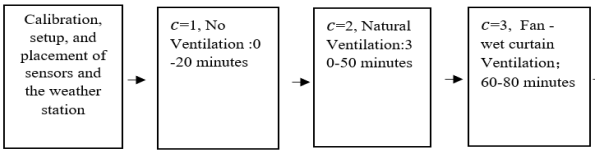

Figure 6: Steps of Ventilation Regulation Time Series Experiment.

Analysis with Comparison Algorithm

To provide a mathematical description of the time-series data analysis and comparison process, the following definitions were established in Table 2 (which includes parameters for the Shading Net Time Series experiment and the Analysis section).

Table 2: Algorithm Parameter List.

Parameters	$\bar{T}_{P(ic)}$	
Meaning	Mean value of a measurement point in a given measurement	
Parameters	c	i
Meaning	Representation of measurement conditions: 1 for No Ventilation; 2 for Natural Ventilation; 3 for Fan-wet curtain ventilation	Measuring points code
Parameters	m	t_{imc}
Meaning	For the count of measurements; c = 1,2,3,4, m = 5; c = 5,6,7, m = 9	Measured values with constant c, i, m
Parameters	$\bar{T}_{oc}$	$\bar{T}_{sc}$
Meaning	Measurement of the average value of the external temperature for corresponding period of time under operating conditions	Average of several specific measurement points for a given measurement
Parameters	n	s
Meaning	Natural numbers, the upper limit of m value for $\bar{T}_{P(ic)}$	Natural numbers, the upper limit of m value for $\bar{T}_{sc}$
Parameters	ΔT_{sc}	
Meaning	Difference between the mean value of all measurement points for a given measurement and the mean value of the external temperature	

In order to complete the experiment data analysis, the following equations needs to be used:

$$\bar{T}_{P(ic)} = \frac{\sum_{m=1}^{n} t_{imc}}{n} \quad (1)$$

$$\bar{T}_{sc} = \frac{\sum_{m=1}^{s} \bar{T}_{P(ic)}}{s} \quad (2)$$

$$\Delta T_{sc} = \bar{T}_{sc} - \bar{T}_{oc} \quad (3)$$

To understand the indoor temperature conditions under each operating state, the analysis was carried out as follows: i), ii), and iii)

i. Temperature Variation and Distribution in the North-South Direction in Greenhouses Under Various Ventilation States

Equation (1) represents the average value of each measurement point, in here, c =1, 2, 3 and i =1, 2, 3, 4, n=5. The experimentally measured values were calculated according to Equation (1), with the calculated values plotted on the vertical axis and the Y-axis coordinates of the measurement points in the greenhouse used as the coordinate values. The resulting comparison curve is shown in Figure 7. By comparing the curves, the temperature distribution in the north-south direction under the four ventilation states showed a pattern of lower temperatures in the south and higher temperatures in the north. However, the cooling capacity of the c = 1 condition was weaker than that of the c = 2 condition, and the cooling

capacity of the c = 3 condition was stronger than both the c = 1 and c = 2 conditions.

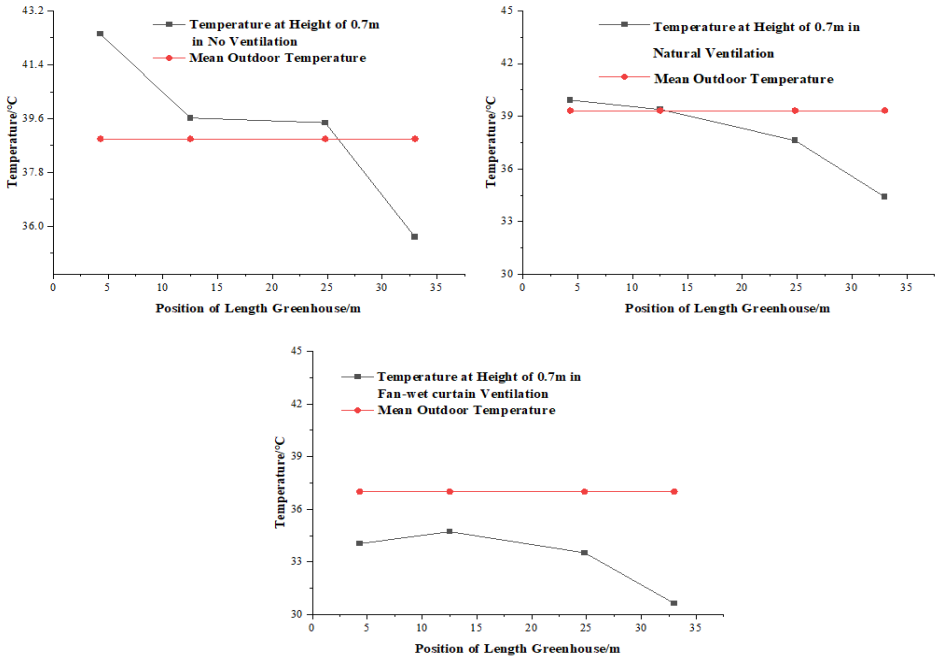

Figure 7: Temperature Variation and Distribution in the North-South Direction in the Greenhouse Under 3 Type Ventilation States.

ii. Temperature Variation and Distribution in the East-West Direction in the Greenhouse Under Various Ventilation Condition

Using Equation (1), where c represents 1, 2, and 3, i corresponds to 5, 3, 4, 7, and n = 5, the average value for each measurement point was calculated. The calculated values were plotted on the vertical axis, with the X-axis coordinates of the measurement points in the greenhouse as the corresponding values. The resulting comparison curve is shown in Figure 8. Upon comparing the curves of the east-west temperature distribution under the four ventilation states, it was observed that the horizontal temperature distribution in the greenhouse generally showed a trend of lower temperatures in the west and higher temperatures in the east.

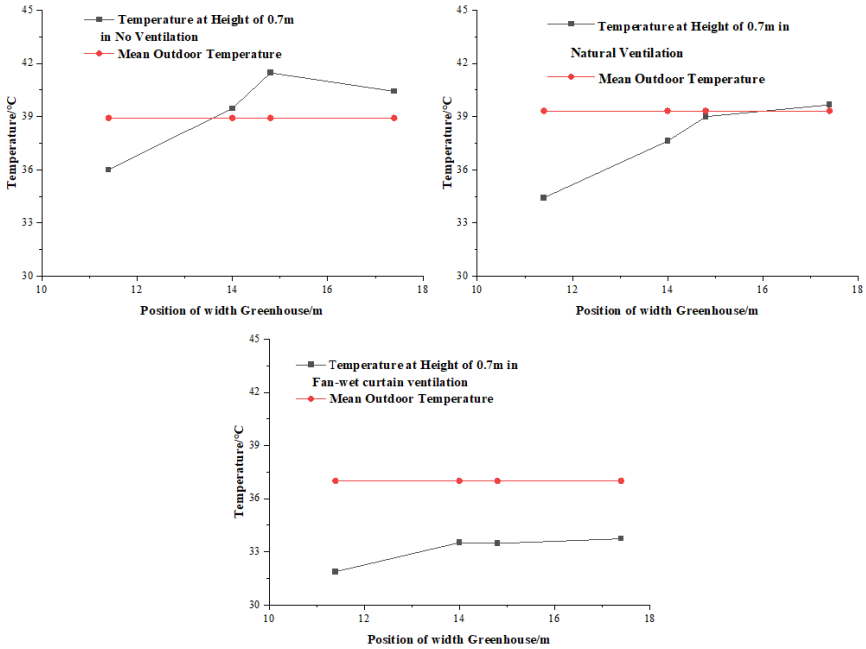

Figure 8: Temperature Variation and Distribution in the East-West Direction in the Greenhouse Under 3 Type Ventilation States.

iii. Temperature Variation and Distribution in the Height Direction in Greenhouses Under Various Ventilation States

Using Equation (1), where c represents 1, 2, and 3, and i ranges from 1 to 21, with n = 5, the average value for each measurement point was calculated. The results were plotted on the vertical axis, with the time of measurement in the greenhouse as the corresponding coordinate value.

The resulting curve is shown in Figure 9. From Figure 9, it is clearly evident from the comparison that, in all four ventilation states, the temperature decreased with height. Mechanical ventilation exhibited significantly better cooling performance, and under condition c = 3, the temperatures at the two heights of 0.7m and 1.3m were similar, though the difference between these values and the temperature at 2.2m was marked in the mechanical ventilation state. Using Equations (1), (2), and (3), the difference between the indoor and outdoor mean temperatures at the three heights was calculated, as shown in Table 3.

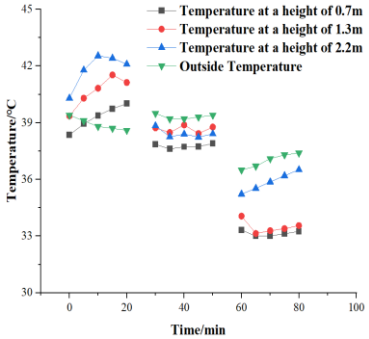

Figure 9: Effect of 3 Types of Ventilation Usage on Indoor Temperature.

Table 3: Difference of the Indoor and Outdoor Mean Values in Three Heights.

Parameters	C=1	C =2	C=3
Height 0.7	-0.72	1.53	4.02
Height 1.3	-2.15	0.63	3.78
Height 2.2	-3.14	0.95	1.10

It was found that the cooling effect of mechanical ventilation was significantly better than that of natural ventilation. At a height of 0.7m in the experimental greenhouse, mechanical ventilation achieved a cooling of up to 4.02°C, while natural ventilation resulted in only 1.53°C of cooling. Furthermore, the cooling effect of natural ventilation was notably better than no ventilation, with no ventilation causing a temperature increase of up to 0.72°C, compared to the 1.53°C cooling achieved with natural ventilation. The height range of the wet curtain was between 0.4 and 1.9m, while the fan's effective range was from 0.3 to 1.7m. Under condition c = 3, mechanical ventilation produced a cooling of 4.02°C at 0.7m and 3.08°C at 1.3m. However, at a height of 2.2m, beyond the influence of mechanical ventilation, the cooling effect reduced to 1.10°C, which was almost identical to the value observed with natural ventilation. This indicates that mechanical ventilation had little impact beyond the height range of the fan and wet curtain, suggesting that the installation height of mechanical ventilation should align with the crop height zone during greenhouse design.

Experiment Methods: Shading Net Time Series Experiment and Analysis

The Shading Net Time Series experiment was conducted as follows:

The layout and setup of the weather station and sensors were identical to those used in the Ventilation Time Series experiment. The greenhouse operated under natural ventilation, with measurements beginning at 2:00 pm, during which the light intensity exceeded 800 W/m². The time series was measured under three different states in the following order: 1. two-layer shading net, 2. one-layer shading net, and 3. no shading net. The values of c for these three operating conditions were 4, 5, and 6, respectively. The specific measurement steps are shown in Figure 10.

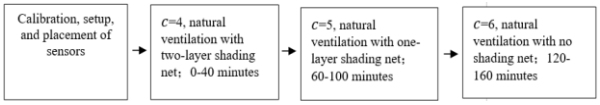

Figure 10: Steps of the Shading Net Time Series Experiment.

Analysis of Shading Net Cooling Experiment

The three measurement points, i = 3, i = 10, and i = 17, located in the central area of the greenhouse, were selected to represent the temperature at heights of 0.7m, 1.3m, and 2.2m during the shading net cooling experiment. Figure 11 shows the temporal changes in the values for i = 3, i = 10, and i = 17, along with a comparison to the outdoor temperature. As shown in the Figure 11, when the shading net was reduced from two layers to one layer, the greenhouse's cooling performance decreased immediately. Furthermore, when the shading net was removed entirely, the cooling performance declined even further. Equation(3) was for calculating the difference between the average temperature inside the greenhouse and the average outdoor temperature, where n is 9, c is 4, 5, 6; i is 1-21, s =21, and $\overline{T}_{P(ic)}$ was from Equation(1), $\overline{T}_{sc}$ was from Equation(2). Under two layers of shading net, the difference ΔT_{sc} was 4.5°C, when it became one layer of shading net, the difference was 3.7°C, and when there was no shading net, the difference was only 1.3°C. The weather station recorded outdoor radiation levels exceeding 800 W/m². The experiment clearly demonstrates that the number of shading net layers significantly impacts the greenhouse's cooling efficiency under high solar radiation during the summer.

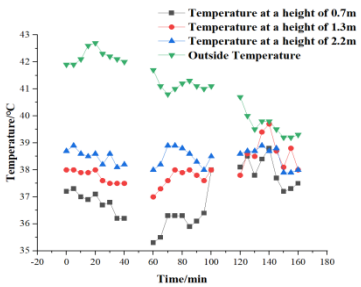

Figure 11: Effect of 3 Types of Shading Net Usage on Indoor Temperature.

Results and Discussion

Simulation Analysis with CFD

To further explore the impact of external airflow on the greenhouse interior, CFD simulations were conducted using Fluent software. A set of instantaneous values corresponding to the condition $c = 4$ was selected as the basis for the simulation setup. The computational domain

used in the simulation was expanded by a factor of ten, as illustrated in Figure 12. In the Fluent simulation, the Energy Equation was enabled, and the Standard Turbulence Model with Standard Wall Functions was selected. Additionally, the Discrete Ordinates radiation model was applied. The latitude and longitude values in the model were set to match the location of the experimental greenhouse. The material properties used in the simulation were specified as outlined in Table 4.

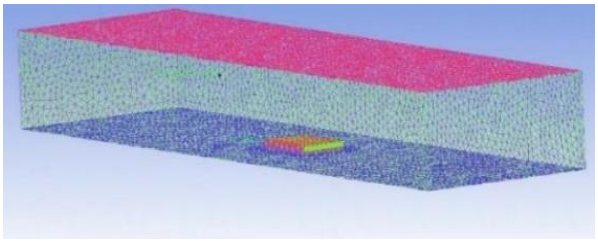

Figure 12: Calculation Domain Settings.

Table 4: Material Properties.

Material Type	Density /kg.m^{-3}	Specific Heat Capacity /Jkg^{-1}.K^{-1}	Thermal Conductivity /Wm.K^{-1}	Absorption Coefficient /m^{-1}	Refract-ion Rate
Concrete	2100	880	1.4	0.6	1.6
Glass	2500	700	0.7	0.1	1.7
Air	1.17	1 025.5	0.03	0	1.0

In the Fluent simulation setup, the calculation domain was configured with the east and south boundaries designated as wind-inlet regions, while the north and west boundaries were set as wind-outlet regions. The wind speed was set to 0.8 m/s, and the wind direction was established at 135°, with the wind direction decomposed into its vector components to ensure an accurate representation of airflow. The inlet temperature was set at 36°C, based on the experimental measurements taken at the site. Additionally, the temperature of the greenhouse walls and floor, both inside and outside, was set according to the experimental data, as detailed in Table 5. To simulate the greenhouse structure accurately, each glass wall was modelled as a translucent wall, allowing for the passage of solar radiation, thereby reflecting the experimental conditions. These settings ensured the simulation closely matched the real-world conditions observed in the greenhouse during the experiment, enabling a more precise analysis of the airflow dynamics and temperature distribution within the environment.

Table 5: Temperatures of Wall and Floor.

Area	Outside Floor	Inside Floor	South Wall	North Wall	East Wall	West Wall	Roof Glass
Temperature/℃	51	43	42	41	42	43	43

The wet curtain side was set as a porous medium, with a permeability α of 2.4 × 10^{-6} m², based on the Fundamental Seepage Law and Bernoulli's Wind-Pressure Relationship (Chevalier et al., 2013). For the shading net, the simulation accounted for radiation discounting based on material parameters from the experimental site. The solar radiation was set to decrease from 821 W/m² to 341 W/m² for the two layers of the shading net, as per the literature and experimental conditions (Abdel-Ghany et al., 2015).

The measured and simulated values for the 21 measurement points are shown in Figure 13. The maximum difference between the greenhouse measured and simulated values is 2.4°C, with a maximum relative error of 6.6%. The minimum difference is 0.1°C, with the most relative error being 0.2%, and the average relative error is 2.5%. The model was validated as usable. A 1m horizontal section at a middle height of 0.7-1.3m was selected to analyse the airflow and temperature distribution.

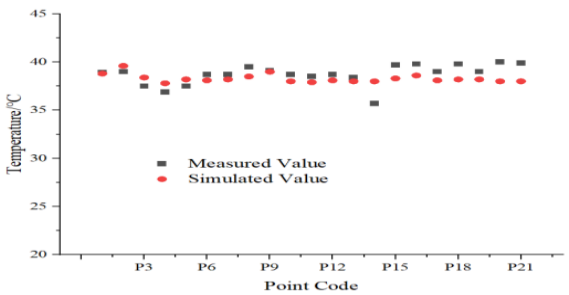

Figure 13: Measured Values and Simulated Values.

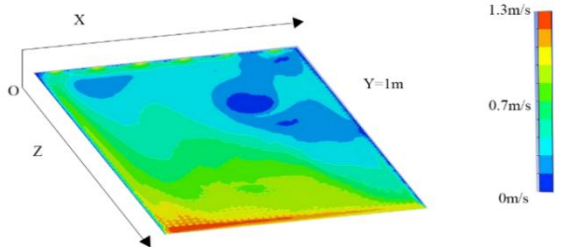

Figure 14: 1m Height Cross-Section Gas Flow.

Figure 14 shows the gas flow cross-section at a height of 1m. It illustrates that the south-east wind entered the greenhouse through the southern wet curtain hole, moving from south to north. This resulted in a lower temperature in the south and a higher temperature in the north. In the east-west direction, due to the absence of side windows on the east and west walls, the south-easterly wind was deflected towards the west, with weaker ventilation towards the east. This created an area of slow airflow on the northeast side of the greenhouse.

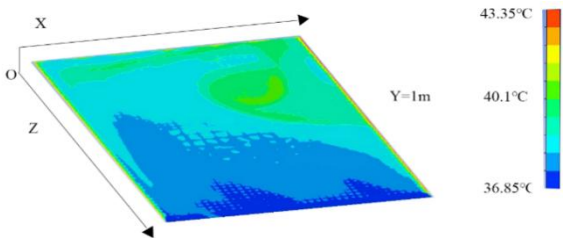

Figure 15: 1m Height Cross-Section Temperature Distribution.

Figure 15 shows the temperature distribution cross-section at a height of 1m, where the greenhouse temperature

exhibits a west-low, east-high trend. The northeast quadrant also shows low temperatures, which aligns with the airflow pattern observed. The simulation results were consistent with the experimental analysis, confirming the accuracy of the temperature distribution. According to the "Standard for Meteorological Parameters of Wind Environment Around Buildings" (Zhuang et al., 2020) issued by China, the prevailing wind direction in the YRD region, represented by Shanghai, is southeast during summer. This confirms that the temperature distribution observed in the greenhouse is representative of the typical characteristics in the YRD region. Figure 16 presents the Wind Rose chart of the average wind direction every 10 minutes during the experiment, showing that the wind predominantly came from the SE region.

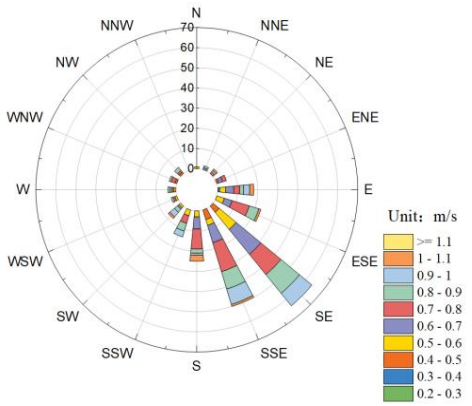

Figure 16: Wind Rose During the Experiment.

Conclusion

The study examined the effects of various temperature control measures, including natural ventilation, fan-wet curtain ventilation, and shading net usage. Based on the analysis and discussion, the following conclusions can be drawn:

i. In glass greenhouses without side windows in the YRD region, the internal temperature distribution during summer follows a general pattern, with temperatures being lower to the south and higher to the north, as well as lower to the west and higher to the east. The cooling is most effective in the southwest quadrant, while the northeast quadrant exhibits poor cooling performance.

ii. In the YRD region, the cooling effect of mechanical ventilation in greenhouses during summer is significantly better than that of natural ventilation, which in turn outperforms the no-ventilation condition. In the experimental greenhouse at a height of 0.7 m, mechanical ventilation reduced the temperature by up to 4.02°C, while natural ventilation achieved a reduction of 1.53°C, and no ventilation resulted in a temperature increase of 0.72°C. The cooling effect of mechanical ventilation is most effective within the installation height range of the fans and wet curtains, and significantly weaker outside these areas.

iii. During high-radiation summer weather, multi-layer shading nets provide a significant cooling effect for greenhouses. When outdoor radiation exceeds 800 W/m², the temperature difference between the average indoor and outdoor temperatures is 4.5°C with two layers of shading net, 3.7°C with one layer, and only 1.3°C with no shading net.

Further strategies for improving summer greenhouse conditions are proposed:

i. Given the temperature distribution of the greenhouse, with lower temperatures to the south and west, and higher temperatures to the north and east, crops requiring more cooling should be planted in the southwest quadrant of the greenhouse. This will help to optimise the cooling efficiency and ensure better crop growth conditions.

ii. Since mechanical ventilation offers a significantly better cooling effect than natural ventilation, and provided energy consumption is manageable, the use of mechanical ventilation is recommended when natural ventilation proves insufficient. Additionally, mechanical ventilation should be installed at heights corresponding to the crop height zone in greenhouse designs.

iii. To maximise cooling in high-radiation summer conditions, multi-layer shading nets should be employed, provided they do not compromise the light levels necessary for plant growth.

References

Abdel-Ghany, A. M., Picuno, P., Al-Helal, I., Alsadon, A., Ibrahim, A., & Shady, M. (2015). Radiometric characterization, solar and thermal radiation in a greenhouse as affected by shading configuration in an arid climate. *Energies*, *8*(12), 13928-13937. doi: https://doi.org/10.3390/en81212404

Ahmed, H. A., Tong, Y.-x., Yang, Q.-c., Al-Faraj, A. A., & Abdel-Ghany, A. M. (2019). Spatial distribution of air temperature and relative humidity in the greenhouse as affected by external shading in arid climates. *Journal of Integrative Agriculture*, *18*(12), 2869-2882. doi: https://doi.org/10.1016/S2095-3119(19)62598-0

Ali, A., & Hassanein, H. S. (2020). Time-Series Prediction for Sensing in Smart Greenhouses. In *GLOBECOM 2020 - 2020 IEEE Global Communications Conference* (pp. 1-6): IEEE. doi: https://doi.org/10.1109/GLOBECOM42002.2020.9322549

Badji, A., Benseddik, A., Bensaha, H., Boukhelifa, A., & Hasrane, I. (2022). Design, technology, and management of greenhouse: A review. *Journal of Cleaner Production*, *373*, 133753. doi: https://doi.org/10.1016/j.jclepro.2022.133753

Cao, Q., Wu, Y., Yang, J., & Yin, J. (2023). Greenhouse temperature prediction based on time-series features and LightGBM. *Applied Sciences*, *13*(3), 1610. doi: https://doi.org/10.3390/app13031610

Chevalier, T., Chevalier, C., Clain, X., Dupla, J. C., Canou, J., Rodts, S., et al. (2013). Darcy's law for yield stress fluid flowing through a porous medium. *Journal of Non-Newtonian Fluid Mechanics*, *195*, 57-66. doi: https://doi.org/10.1016/j.jnnfm.2012.12.005

Chiboub, H., Abid, H., Lajnef, M., Zouari, S., Gugliuzza, G., Mejri, M., et al. (2024). The impact of mechanical ventilation on Sfax City's greenhouse microclimate. *CFD Letters*, *16*(8), 150-162. doi:

https://doi.org/10.37934/cfdl.16.8.150162

Choi, Y.-B., Kim, R.-W., & Lee, I.-b. (2024). Numerical analysis of snow distribution on greenhouse roofs using CFD–DEM coupling method. *Biosystems Engineering*, *237*, 196-213. doi: https://doi.org/10.1016/j.biosystemseng.2023.09.018

Fan, Y., Jin, X., Gan, L., Yang, Q., Wang, L., Lyu, L., et al. (2023). Exploring an integrated framework for "dynamic-mechanism-clustering" of multiple cultivated land functions in the Yangtze River Delta region. *Applied Geography*, *159*, 103061. doi: https://doi.org/10.1016/j.apgeog.2023.103061

Feng, C., Yuan, G., Wang, R., Chen, X., Ma, F., Yang, H., et al. (2024). Performance study on a novel greenhouse cover structure with beam split and heat control function. *Energy Conversion and Management*, *301*, 118077. doi: https://doi.org/10.1016/j.enconman.2024.118077

Flores-Velazquez, J., Montero, J. I., Baeza, E. J., & Lopez, J. C. (2014). Mechanical and natural ventilation systems in a greenhouse designed using computational fluid dynamics. *International Journal of Agricultural and Biological Engineering*, *7*(1), 1-16. doi: https://doi.org/10.3965/j.ijabe.20140701.001

Ganguly, A., & Ghosh, S. (2011). A review of ventilation and cooling technologies in agricultural greenhouse application. *Iranica Journal of Energy & Environment*, *2*(1), 32-46. Retrieved from https://www.ijee.net/article_64325_ed4445b59a403b945cb9d541465c6a5f.pdf

Ghani, S., El-Bialy, E. M. A. A., Bakochristou, F., Mohamed Rashwan, M., Mohamed Abdelhalim, A., Mohammad Ismail, S., et al. (2020). Experimental and numerical investigation of the thermal performance of evaporative cooled greenhouses in hot and arid climates. *Science and Technology for the Built Environment*, *26*(2), 141-160. doi: https://doi.org/10.1080/23744731.2019.1634421

Ludwig, S. A. (2019). Comparison of Time Series Approaches applied to Greenhouse Gas Analysis: ANFIS, RNN, and LSTM. In *2019 IEEE International Conference on Fuzzy Systems (FUZZ-IEEE)* (pp. 1-6). https://doi.org/10.1109/FUZZ-IEEE.2019.8859013

Lyu, X., Xu, Y., Wei, M., Wang, C., Zhang, G., & Wang, S. (2022). Effects of vent opening, wind speed, and crop height on microenvironment in three-span arched greenhouse under natural ventilation. *Computers and Electronics in Agriculture*, *201*, 107326. doi: https://doi.org/10.1016/j.compag.2022.107326

Nomura, K., Saito, M., Tada, I., Iwao, T., Yamazaki, T., Kira, N., et al. (2022). Estimation of photosynthesis loss due to greenhouse superstructures and shade nets: A case study with paprika and tomato canopies. *HortScience*, *57*(3), 464-471. doi: https://doi.org/10.21273/HORTSCI16384-21

Odhiambo, M. R., Abbas, A., Wang, X., & Mutinda, G. (2020). Solar energy potential in the Yangtze River delta region—A GIS-based assessment. *Energies*, *14*(1), 143. doi: https://doi.org/10.3390/en14010143

Villagrán, E., Flores-Velazquez, J., Akrami, M., & Bojacá, C. (2021). Influence of the height in a Colombian multi-tunnel greenhouse on natural ventilation and thermal behavior: Modeling approach. *Sustainability*, *13*(24), 13631. doi: https://doi.org/10.3390/su132413631

Wang, C., Nan, B., Wang, T., Bai, Y., & Li, Y. (2021). Wind pressure acting on greenhouses: A review. *International Journal of Agricultural and Biological Engineering*, *14*(2), 1-8. doi: https://doi.org/10.25165/j.ijabe.20211402.5261

Wang Xinzhong, e. a. (2016). Analysis of flow field for full open-roof glass greenhouse with nature ventilation in summer based on CFD. *Transactions of the Chinese Society for Agricultural Machinery*, *47*(10), 332-337. doi: http://doi.org/10.6041/j.issn.1000-1298.2016.10.042

Zhuang, Z., Che, X., Wang, Y., Yao, J., Li, C., & Xu, W. (2020). *Shanghai Engineering Building Code: Standard for Meteorological Paramters of Wind Environment Around Buildings*: Shanghai: Tongji University Press.